AIP | Applied Physics Letters

On-chip non-reciprocal optical devices based on quantum inspired photonic lattices

R. El-Ganainy, A. Eisfeld, Miguel Levy, and D. N. Christodoulides

Citation: Appl. Phys. Lett. **103**, 161105 (2013); doi: 10.1063/1.4824895
View online: http://dx.doi.org/10.1063/1.4824895
View Table of Contents: http://apl.aip.org/resource/1/APPLAB/v103/i16
Published by the AIP Publishing LLC.

On-chip non-reciprocal optical devices based on quantum inspired photonic lattices

R. El-Ganainy,[1,2,a)] A. Eisfeld,[1] Miguel Levy,[2] and D. N. Christodoulides[3]
[1]*Max Planck Institute for the Physics of Complex Systems, Nothnitzer Street 38, 01187 Dresden, Germany*
[2]*Department of Physics, Michigan Technological University, Houghton, Michigan 49931, USA*
[3]*College of Optics and Photonics-CREOL, University of Central Florida, Orlando, Florida 32816, USA*

(Received 30 May 2013; accepted 22 September 2013; published online 14 October 2013)

We propose integrated optical structures that can be used as isolators and polarization splitters based on engineered photonic lattices. Starting from optical waveguide arrays that mimic Fock space (quantum state with a well-defined particle number) representation of a non-interacting two-site Bose Hubbard Hamiltonian, we show that introducing magneto-optic nonreciprocity to these structures leads to a superior optical isolation performance. In the forward propagation direction, an input TM polarized beam experiences a perfect state transfer between the input and output waveguide channels while surface Bloch oscillations block the backward transmission between the same ports. Our analysis indicates a large isolation ratio of 75 dB after a propagation distance of 8 mm inside seven coupled waveguides. Moreover, we demonstrate that, a judicious choice of the nonreciprocity in this same geometry can lead to perfect polarization splitting. © *2013 AIP Publishing LLC*. [http://dx.doi.org/10.1063/1.4824895]

Integrated optics is playing an ever increasingly important role in modern technology. From communication networks to medical applications, photonic devices are becoming vital elements in every commercial system where their different functionalities are enabled by variety of physical and engineering concepts. The viability of these photonic devices depends on several important parameters such as fabrication tolerances, compatibility with existing technologies, power management, and versatility. While the last decade has witnessed rapid developments in miniaturizing photonic components, realization of high performance commercial on-chip optical isolators still remains a hurdle. These devices operate as optical diodes that allow unidirectional transmission of light and they are essential components in most optical systems.

Proper operation of optical isolators necessitates large isolation ratios of at least 30 dB, low insertion loss, and negligible optical absorption. In order to satisfy the aforementioned requirements, today's commercial isolators are based on Faraday rotation.[1] However, these devices suffer from the major drawback of being bulky and incompatible with integrated optical platforms. Attempts to overcome this difficulty have led to a surge of new ideas and concepts for designing integrated optics isolators. These investigations range from using integrated magneto-optics material,[2,3] acoustic/electro-optics effects,[4] and Kerr nonlinearity[5] to non-Hermitian optics.[6] Optical diodes based on nonreciprocal silicon rings have been also reported.[7]

Recently, optical isolators based on unidirectional optical Bloch oscillations (BO) were proposed and 35 dB isolation ratios were predicted in simulations.[8–10] Following this work, it was shown in simulations that non-reciprocal resonant delocalization (RD) effects[11,12] can lead to an even higher performance (45 dB) and smaller footprint.[12] Despite the characteristic advantages and limitations of each of the above techniques, the non-reciprocal Bloch oscillations are emerging as a very promising paradigm for realizing on-chip optical diodes. For instance, it is compatible with mature silicon-on-insulator (SOI) technologies[8–10] and does not depend on any nonlinear processes that might degrade the performance at low input powers. In addition, it is based on waveguide transmission structures, and thus, it enjoys a large bandwidth of operation.[13] Moreover, careful waveguide coupling can minimize insertion loss in these geometries. Finally, we note that their operation requires small magnetic effects (compared with those used in commercial isolators based on Faraday rotation) that can be provided using thin film magnetic garnets.[8]

In this Letter, we propose high performance integrated optical isolators based on quantum inspired uniform non-reciprocal waveguide lattices with inhomogeneous coupling constants. In contrast to Ref. 12, the proposed geometry does not involve modulation of the waveguide width along the propagation direction and is thus easier to fabricate. In addition, it achieves a much superior performance to those reported in Refs. 8 and 12. Even more importantly, we demonstrate the versatility of our proposed device by showing that it can be used as a polarization splitter. The operation of this photonic diode is based on a complete transfer of optical intensity from one waveguide site at the input to another channel at the output during forward propagation. On the other hand, surface revival effects block any backward propagation to the input waveguide element, thus providing optical isolation.

Figure 1 shows a schematic of the proposed optical isolator. It consists of waveguide array with varying widths and/or heights. A magnetic film layer (not shown in Fig. 1) is deposited on top of the waveguide array.[8–10] The dimensions of the waveguide elements together with the thickness of the magnetic film and the strength of the applied magnetic field are chosen to ensure a linear propagation constant ramp of $\Delta\beta$ in the backward propagation direction while keeping the

a)ganainy@mtu.edu

array unbiased ($\Delta\beta = 0$) in the forward propagation.[8–10] Moreover, the coupling coefficients between adjacent channels are not constant but rather follow a square root pattern. Within the context of electromagnetic coupled mode theory, the electric field modal values $E_n(z)$ obey the coupled mode equations[14]

$$\begin{aligned} i\frac{dE_{-N}}{dz} &= -\Delta\beta N E_{-N} + \kappa\sqrt{2N}E_{-N+1}, \\ i\frac{dE_n}{dz} &= \Delta\beta n E_n + \kappa(g_n E_{n-1} + g_{n+1}E_{n+1}), \quad -N < n < N, \\ i\frac{dE_N}{dz} &= \Delta\beta N E_N + \kappa\sqrt{2N}E_{N-1}, \end{aligned} \tag{1}$$

where $g_n = \sqrt{(N+n)(N-n+1)}$ and κ is a parameter that determines the coupling constants. Note that the number of waveguides is assumed to be $2N+1$ and these are labeled according to $-N \le n \le N$.

Equation (1) describes both the forward ($\Delta\beta = 0$) and backward ($\Delta\beta \neq 0$) propagation dynamics of any indicant optical beam and is used to evaluate the performance of the proposed optical diode.

Note that the square root variation of the coupling coefficients is inspired by Fock space representations of two coupled bosonic modes.[15] Within this context, Eq. (1) can be investigated analytically and stationary solutions having the form $E_n(z) = A_n \exp(i\lambda_{2N+1,n}z)$ can be obtained in closed form.[15] Most notably, the eigenvalues are equidistant and are given by

$$\lambda_{2N+1,n} = n\sqrt{(\Delta\beta)^2 + 4\kappa^2}, \tag{2}$$

where the subscript $2N+1$ refers to the number of waveguides and n is the eigenmode index. The equidistant ladder distribution of the eigenvalue spectrum together with the mirror symmetry around the middle waveguide element when $\Delta\beta = 0$ lead to perfect state transfer (complete transfer of excitation from one input channel to a different waveguide element at the output).[16,17] On the other hand, introducing a nonzero $\Delta\beta$ breaks the mirror symmetry around the middle channel while preserving the constant eigenvalue gradient, thus leading to surface revivals (the spread and refocusing of an input beam launched at the edge of the array).[18]

For concreteness, we consider a system operating at the telecommunication wavelength of $\lambda = 1.55\,\mu$m and made of 7 waveguide elements (i.e., $N = 3$) and $\kappa = 7/\sqrt{12}\,\text{cm}^{-1}$. Consequently, the coupling coefficients of the array take the values: $7 \times [1/\sqrt{2} \quad \sqrt{5/6} \quad 1 \quad 1 \quad \sqrt{5/6} \quad 1/\sqrt{2}]\ \text{cm}^{-1}$. Finally, for this particular example, the backward ramp in the propagation is chosen as $\Delta\beta = 0.82 \times 7\,\text{cm}^{-1} = 5.74\ \text{cm}^{-1}$. There are different ways of implementing these parameters. For example, 800 nm-wide, 300 nm-thick silicon-on-insulator ridge waveguides with cerium-substituted yttrium-iron-garnet cover-layers separated center-to-center by 1.61 μm, 1.575 μm, and 1.56 μm, respectively, produce the required coupling coefficients to within 3% (beam-propagation simulation). Ridge-thickness differences of ~20 nm between adjacent ~300 nm-thick waveguide ridges produce nonreciprocal-phase-shift gradients $5.75 \pm 0.05\ \text{cm}^{-1}$.[19] The same can be obtained by composition (gyrotropy) gradients in the iron-garnet cover layers across the ridge-waveguide array. A garnet cover-layer thickness of ~100 nm is sufficient to induce nonreciprocal operation.[20] This layer is in-plane magnetized transversely to the propagation direction.

Fig. 2 depicts the evolution dynamics of the electric field modal intensity $|E_n(z)|^2$ in each waveguide element in both forward and backward propagation directions. These results are obtained numerically by using the above mentioned physical parameters in Eq. (1) and the simulations are carried out using Runge-Kutta scheme. As shown in Fig. 2(a), an input beam launched at the left most waveguide will undergo a complete state transfer[17] (all optical power is transferred to the right most waveguide) after a propagation distance given by $L = \pi/(2\kappa) \approx 7.8$ mm. On the other hand, a backward reflected beam will experience an effectively "tilted" array due to the propagation constant ramp. As a result surface revival effects take place with a revival period of $D = \pi/\sqrt{\left(\frac{\Delta\beta}{2}\right)^2 + \kappa^2} \approx 9$ mm. Under these conditions, our numerical analysis shows that most of the backward optical power exits from the right most waveguides and a large isolation ratio of ~75 dB is numerically predicted.

We note that this is a dramatic improvement over the previous results obtained using waveguide arrays with uniform coupling. Moreover, our analysis indicates a profound performance when $\Delta\beta = 7\,\text{cm}^{-1}$. In the latter scenario, all the

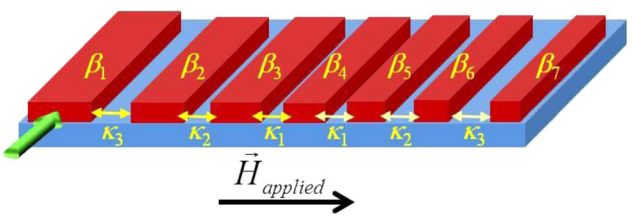

FIG. 1. A schematic of coupled waveguide array used as optical diode. The width and/or height of each waveguide elements are carefully designed to introduce a linear ramp in the propagation constant in the backward direction. Nonreciprocal effects are introduced into the structure by depositing magnetic garnet films (not shown here) on top of each waveguide channel such that a forward propagating optical beam will experience a zero index gradient.

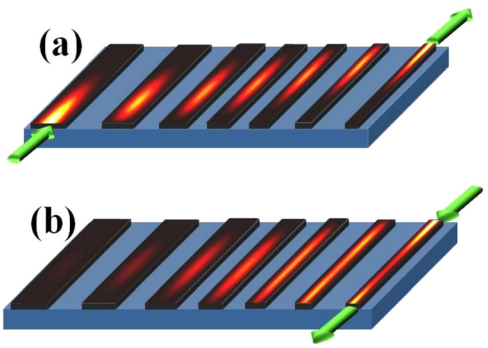

FIG. 2. A schematic of the proposed optical isolator structure showing the evolution of the modal electric field intensity $|E_n(z)|^2$. The array consists of 7 waveguide elements with $\kappa = 7/\sqrt{12}\,\text{cm}^{-1}$. (a) For $\Delta\beta = 0$, complete state transfer is achieved in the forward direction where an input optical beam in the left most waveguide will exit from the right most channel after 7.8 mm of propagation. (b) Surface revival effects dominate in the backward propagation when $\Delta\beta = 5.74\ \text{cm}^{-1}$ and high isolation ratio of 75 dB is obtained numerically.

backward optical power exits from the right most waveguide with null output from the left most channel and a perfect isolation is achieved. Note however that this requires a 22% increase in the degree of the nonreciprocity. In practice, 75 dB isolation is very large and together with a smaller degree of nonreciprocity might be preferable to a perfect isolation.

The prediction of such a high degree of isolation elevates the upper limit on the isolator performance. It also indicates that given a suitable mechanism for controlling the garnet films magnetism, one might be able to use the device as a switch to direct input beams to either one of the two output channels (left/right most waveguides). This merits further investigation and we will carry out this study elsewhere.

Finally, we now illustrate that this perfect isolation regime can be used for polarization splitting. In order to do so, we note that while all the previous analysis applies only for TM polarized light,[8–10] TE modes are not affected by the garnet films magnetization (in the direction shown by the black arrow labeled $\vec{H}_{app}$ in Fig. 1).

Let us now consider an input beam composed of a superposition of TM/TE modes. This scenario is depicted in Fig. 3, where again we plot the electric field modal intensity $|E_n(z)|^2$obtained by numerical integration (using Runge-Kutta method) of Eq. (1) for the same physical parameters used in Fig. 2. Note that, for illustration purposes, the propagation of the two superimposed polarizations is separated into two sub-plots. As shown in the bottom (green) part of Fig. 3, the TM mode "sees" a uniform lattice, and its optical power is fully transferred to the opposite side of the array. On the other hand, the TE mode will be subject to the lattice "tilt" and surface revivals takes over. Thus, the output TE power exits from the same input channel as depicted in the upper subplot of Fig. 3. As a result, a perfect splitting between the two states of polarization is achieved.

We note that several proposals for TE/TM splitting have been suggested and demonstrated in the literature (see, for example, Refs. 21 and 22). The obvious advantages of the design presented here lie in its high performance and its compatibility with optical isolator designs. In other words, the same structure can have dual functionality. This last feature is extremely important and provides a tremendous advantage for integrated optics industry, namely, that same fabrication techniques and facilities can be used without any modifications to build two different devices. Hence, not only our proposed design provides an avenue for high performance devices but it also offers a great opportunity for low cost fabrication.

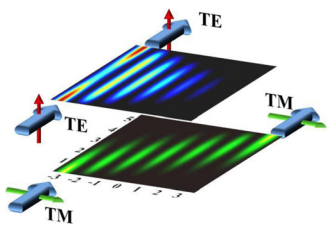

FIG. 3. On-chip polarization splitter. Both subplots depict the evolution of the optical intensity $|E_n(z)|^2$of an optical beam composed of two orthogonal TE/TM polarizations launched in the left most waveguide element. Due to its sensitivity to the magneto-optic effects, the TM mode experiences a uniform array and undergoes a perfect state transfer as shown in the bottom part of the figure. On the other hand, the TE polarization can sense the lattice tilt and exits from the same input channel as shown on the top figure. Small arrows (in red and green) indicate the transverse component of the magnetic field of the modes.

In conclusion, we have proposed integrated optical structures that can be used as isolators and polarization splitters based on engineered photonic lattices. The design parameters of such geometries were inspired by Fock space representation of a non-interacting two-site Bose Hubbard Hamiltonian. We have shown that introducing magneto-optic nonreciprocity to these structures leads to a superior optical isolation performance of 75 dB after a propagation distance of 8 mm inside seven coupled waveguides. In the forward propagation direction, an input TM polarized beam experiences a perfect state transfer between the input and output waveguide channels while surface Bloch oscillations block the backward transmission between the same ports. Moreover, we have demonstrated that the same structure can operate as a perfect polarization splitter.

[1]B. A. E. Saleh and M. C. Teich, *Fundamentals of Photonics* (John Wiley & Sons, New Jersey, 1991).
[2]M. Levy, R. M. Osgood, Jr., H. Hegde, F. J. Cadieu, R. Wolfe, and V. J. Fratello, IEEE Photon. Technol. Lett. **8**, 903–905 (1996).
[3]J. Fujita, M. Levy, R. M. Osgood, Jr., L. Wilkens, and H. Dotsch, Appl. Phys. Lett. **76**, 2158–2160 (2000).
[4]Z. Yu and S. Fan, Nature Photon. **3**, 91–94 (2009).
[5]L. Fan, J. Wang, L. T. Varghese, H. Shen, B. Niu, Y. Xuan, A. M. Weiner, and M. Qi, Science **335**, 447 (2012).
[6]H. Ramezani, T. Kottos, R. El-Ganainy, and D. N. Christodoulides, Phys. Rev. A **82**, 043803 (2010).
[7]M.-C. Tien, T. Mizumoto, P. Pintus, H. Kromer, and J. E. Bowers, Opt. Express **19**, 11740–11745 (2011).
[8]M. Levy and P. Kumar, Opt. Lett. **35**, 3147 (2010).
[9]P. Kumar and M. Levy, Opt. Lett. **36**, 4359 (2011).
[10]P. Kumar and M. Levy, Opt. Lett. **37**, 3762 (2012).
[11]R. El-Ganainy, D. N. Christodoulides, C. E. Rüter, and D. Kip, Opt. Lett. **36**, 1464 (2011).
[12]R. El-Ganainy, P. Kumar, and M. Levy, Opt. Lett. **38**, 61 (2013).
[13]A Szameit, I. L. Garanovich, M. Heinrich, A. A. Sukhorukov, F. Dreisow, T. Pertsch, S. Nolte, A. Tünnermann, and Y. S. Kivshar, Nat. Phys. **5**, 271 (2009).
[14]K. Okamoto, *Fundamentals of Optical Waveguides* (Academic Press, Burlington, 2005).
[15]See supplementary material at http://dx.doi.org/10.1063/1.4824895 for more details on the analytical solution of Eq. (1).
[16]M. Christandl, N. Datta, A. Ekert, and A. J. Landahl, Phys. Rev. Lett. **92**, 187902 (2004).
[17]A. Perez-Leija, R. Keil, A. Kay, H. Moya-Cessa, S. Nolte, L. C. Kwek, B. M. Rodríguez-Lara, A. Szameit, and D. N. Christodoulides, Phys. Rev. A **87**, 012309 (2013).
[18]R. Keil, A. Perez-Leija, P. Aleahmad, H. Moya-Cessa, S. Nolte, D. N. Christodoulides, and A. Szameit, Opt. Lett. **37**, 3801 (2012).
[19]R. L. Espinola, T. Izuhara, M.-C. Tsai, R. M. Osgood, Jr., and H. Dötsch, Opt. Lett. **29**, 941–943 (2004).
[20]L. Bi, J. Hu, P. Jiang, D. H. Kim, G. F. Dionne, L. C. Kimerling, and C. A. Ross, Nature Photon. **5**, 758–762 (2011).
[21]H. Fukuda, K. Yamada, T. Tsuchizawa, T. Watanabe, H. Shinojima, and S. Itabashi, Opt. Express **14**, 12401 (2006).
[22]H. Chong, P. I. Borel, L. H. Frandsen, R. M. De La Rue, and R. Baets, IEEE Photon. Technol. Lett. **15**, 1249 (2003).